Manipulating Dirac states in BaNiS_2 by surface charge doping

Jiuxiang Zhang, Thibault Daniel Pierre Sohier, Michele Casula, Zhesheng Chen, Jonathan Caillaux, Evangelos Papalazarou, Luca Perfetti, Luca Petaccia, Azzedine Bendounan, Amina Taleb-Ibrahimi, et al.

Manipulating Dirac states in $BaNiS_2$ by surface charge doping

Jiuxiang Zhang,[†] Thibault Sohier,[‡] Michele Casula,[¶] Zhesheng Chen,[†] Jonathan Caillaux,[†] Evangelos Papalazarou,[†] Luca Perfetti,[§] Luca Petaccia,[‖] Azzedine Bendounan,[⊥] Amina Taleb-Ibrahimi,[⊥] David Santos-Cottin,[¶] Yannick Klein,[¶] Andrea Gauzzi,[¶] and Marino Marsi[*,†]

†*Université Paris-Saclay, CNRS, Laboratoire de Physique des Solides, 91405, Orsay, France*

‡*Laboratoire Charles Coulomb (L2C), Université de Montpellier, CNRS, Montpellier, France*

¶*IMPMC, Sorbonne Université, CNRS, IRD, MNHN, 75252, Paris, France*

§*Laboratoire des Solides Irradiés, Ecole Polytechnique, CNRS-UMR 7642, CEA, 91128, Palaiseau, France*

‖*Elettra Sincrotrone Trieste, Strada Statale 14 km 163.5, 34149, Trieste, Italy*

⊥*Synchrotron SOLEIL, L'Orme des Merisiers, BP 48 Saint-Aubin, 91192, Gif-sur-Yvette Cedex, France*

E-mail: marino.marsi@universite-paris-saclay.fr

Abstract

In the Dirac semimetal $BaNiS_2$, the Dirac nodes are located along the $\Gamma - M$ symmetry line of the Brillouin zone, instead of being pinned at fixed high-symmetry points. We take advantage of this peculiar feature to demonstrate the possibility of moving the Dirac bands along the $\Gamma - M$ symmetry line in reciprocal space by varying the concentration of K atoms adsorbed onto the surface of cleaved $BaNiS_2$ single crystals. By means of first-principles calculations, we give full account for this observation by considering the effect of the electrons donated by the K atom on the charge transfer gap, which establishes a promising tool for engineering Dirac states at surfaces, interfaces and heterostructures.

Keywords

Dirac materials, time-resolved ARPES, $BaNiS_2$, charge transfer gap, surface electron doping

Introduction

During the last decades, an intensive experimental and theoretical effort has led to the discovery of a variety of novel materials hosting electronic states with nontrivial topological properties. Among these states, linearly dispersing bands crossing at the Fermi level,[1] called 'Dirac cones', have attracted a great deal of interest due to their unique semimetallic properties, such as very high carrier mobility, promising for novel concepts of electronic devices. A prerequisite for these developments is the control of the Dirac states, which is not possible in most materials including archetypal graphene, where the Dirac nodal points are pinned at high-symmetry points of the Brillouin zone due to the constraints set by crystal symmetry. New perspectives have been disclosed by the discovery of materials with unpinned Dirac cones, like the surface of ZrSnTe,[2] atomic layers, e.g. Sb,[3] transition metal dichalcogenides[4] and nonsymmorphic layered compounds, such as ZrSiS[5] and $BaNiS_2$.[6]

In this letter, we consider $BaNiS_2$, a prototype of correlated Dirac semimetal where the Dirac states are located along the $\Gamma - M$ symmetry line.[7] Our motivation is that, in this system, the band inversion mechanism and the Dirac cone formation are determined by the $p - d$ hybridization and by the charge transfer gap; hence, the cones can be moved along the above symmetry line by partially substituting Ni for Co, for this substitution alters both properties, as demonstrated recently.[6] Specifically, by increasing the Ni concentration, x, in $BaCo_{1-x}Ni_xS_2$, the cones move away from Γ and shift down in energy. Note that x is also a control parameter of the strength of the electronic correlations that govern a remarkable Mott metal-insulator transition[8–10] and the spin-orbit coupling.[11,12] All these results show that chemical substitution is an effective tool to manipulate Dirac states in $BaCo_{1-x}Ni_xS_2$ and that charge transfer is an essential control parameter.

In the present work, we use alkali metal deposition on the surface as an alternative approach to manipulate the Dirac states of $BaNiS_2$. Indeed, adsorbed alkali metal atoms are prone to donate valence electrons to the surface, which has been commonly used to tune carrier concentration in semiconductor substrates. Such extra electrons induce a band bending at the surface, thus filling the surface conduction electronic states that are normally empty in the bulk. This effect is produced by the dipolar electric field created at the surface by the charge transfer. As discussed in previous studies, surface doping effects have been exploited to modify effectively the band structure of various substrate materials.[13,14]

By combining conventional angle-resolved photoemission spectroscopy (ARPES) and pump-probe, time-resolved ARPES experiments with first-principles calculations, we succeeded in probing *in situ* and explaining theoretically the effects of surface doping on the electronic structure of $BaNiS_2$. Figure 1 illustrates a schematic layout of the experimental set-up used. We find that the Dirac cones move towards Γ and shift down in energy with increasing K coverage, which is explained by a modification of the $p - d$ hybridization gap induced by the electrostatic dipolar field produced by surface doping. These results indicate a viable approach to control Dirac states in a variety of two-dimensional materials and to

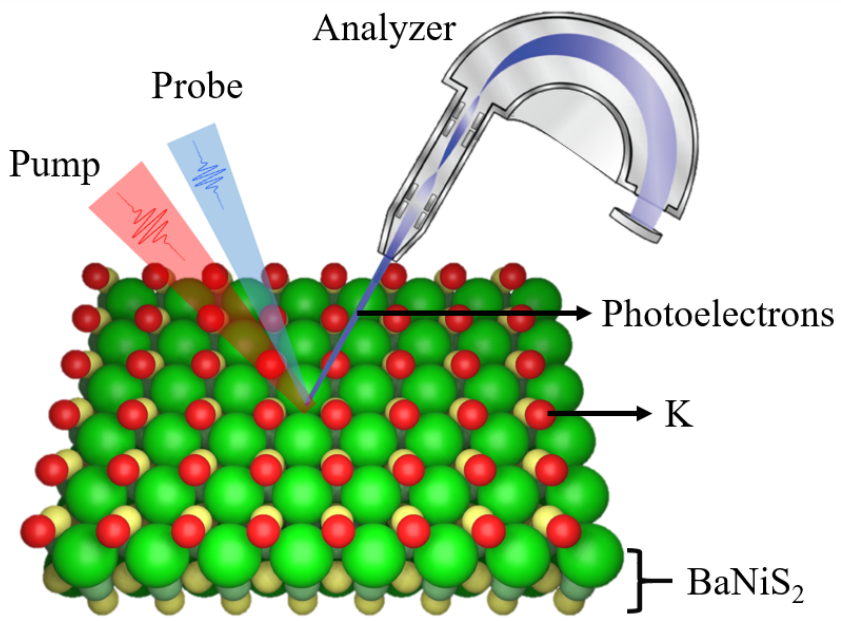

Figure 1: Schematic of the time-resolved ARPES measurement on $BaNiS_2$ with *in situ* surface K doping.

functionalize these states in view of practical electronic applications.

Results

Figures 2(a),(b) and (c) illustrate the evolution of the band structure of $BaNiS_2$ measured by ARPES after each K evaporation step using a photon energy of 25 eV. During the evaporation and the measurements, the temperature of the $BaNiS_2$ substrate was kept at low temperature (about 100 K). The present data confirm a previous ARPES study[7] that unveiled a Fermi surface formed by an electron pocket at Γ and by a Dirac cone located along the ΓM direction. The above previous study also confirmed the *d*-orbital nature of the Dirac bands. In order to evaluate the amount of adsorbed K after each evaporation, we monitored the evolution of the intensities of the core level peaks from the substrate (Ba 5p) and from the K overlayer (K 3p) with K evaporation time. The binding energy of both orbitals being of about 18 eV, we used a 31 eV photon energy. The result is shown in Figure 2(d). As expected, we find that the intensity of the K 3*p* peak increases while the intensity of Ba 5*p* peaks decreases.

Considering that K and Ba have similar cross sections for photon energies around 30 eV [15,16] and taking into account the photoelectron escape depth at this energy, we estimate that 20 minutes of evaporation corresponds to the deposition of 1 ML of K.

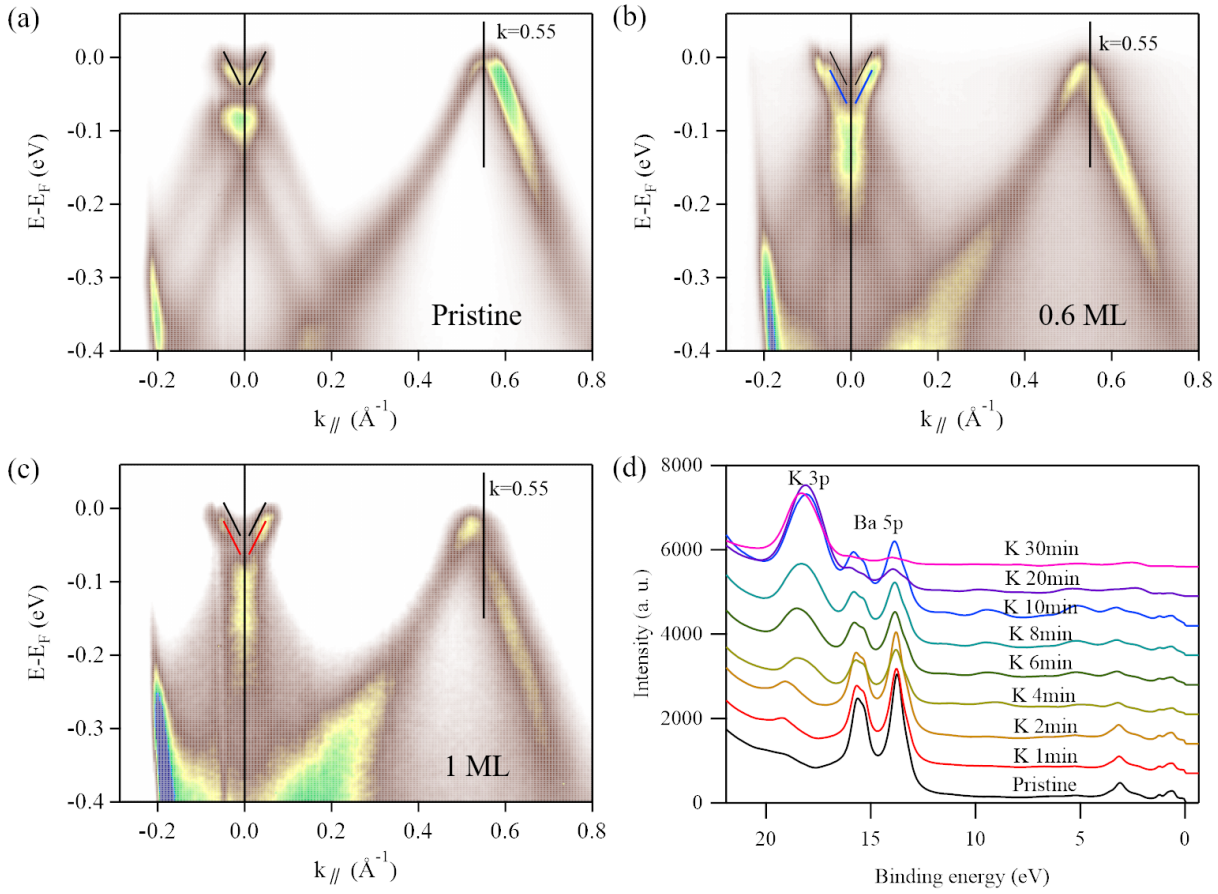

Figure 2: ARPES spectra (25 eV photon energy) for the evolution of the band structure of $BaNiS_2$ with surface K dosing. (a) Pristine surface. After deposition of 0.6 (b) and 1 (c) K monolayers (c). (d) The evolution of the core levels of $BaNiS_2$ with surface K dosing (data taken using 31 eV photon energy). All the data were taken at about 100 K.

In Figure 2, one notes that, upon K deposition, the spectroscopic features of the $BaNiS_2$ substrate become less sharp but remain still visible; we observe two clear trends: (i) a downwards shift in energy of all electronic bands, as expected in the case of electron transfer from an adsorbed alkali metal atom; (ii) a systematic shift in k-position of the Dirac cone towards Γ with increasing alkali metal coverage (or electron doping). This shift is evident by comparing the position of the Dirac node, determined by extrapolating the linear dispersion

of the Dirac bands, in Figures 2(a),(b) and (c).

Indeed, in $BaNiS_2$, the Dirac points are slightly above the Fermi level, so they cannot be directly detected with ARPES. In order to determine more precisely their position and hence the above k-shifts, we successfully employed time-resolved (TR-) ARPES. The reason is that the pump-probe technique enables to detect electronic states above the Fermi energy.[17] A further advantage of laser-based TR-ARPES is the higher momentum resolution at low photon energy (6.28 eV), which improves the accuracy of the k-shift measurement. The results of the TR-ARPES study are summarized in Figure 3(a)-(d), where we plot the pump-probe data measured at the delay time of +200 fs which corresponds to the maximum intensity for the photoexcited states. Figure 3(e) shows the shift of two branches of the Dirac cone after selected K deposition times. In Figure 3(f) we plot the evolution of the Dirac point position with increasing surface doping level, expressed as K coverage.

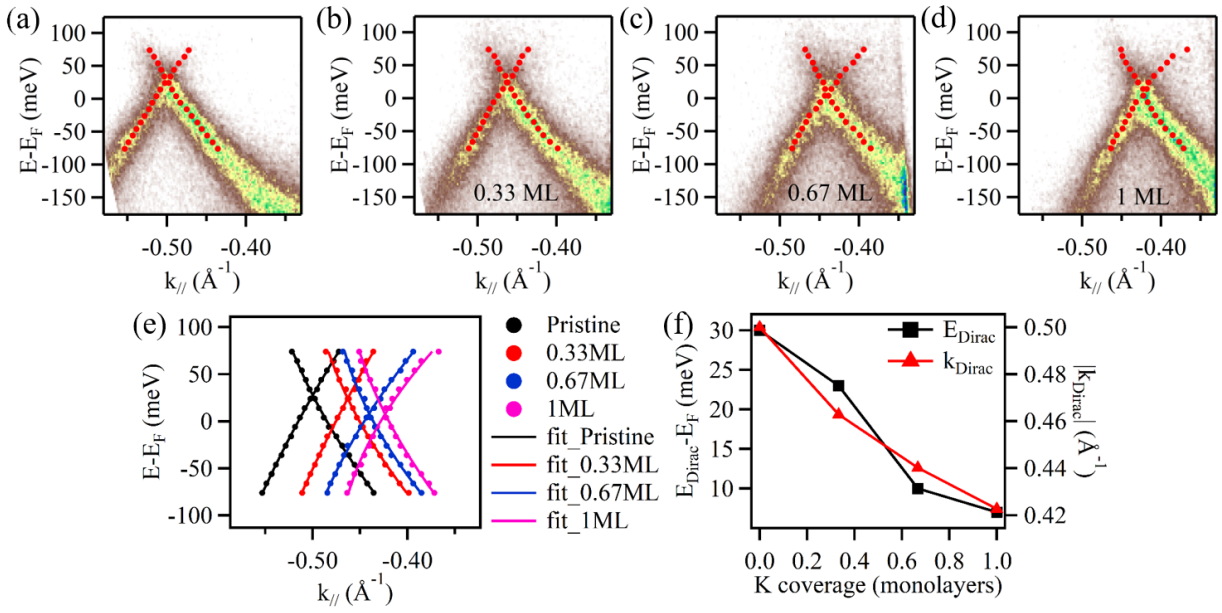

Figure 3: Evolution of the Dirac states of $BaNiS_2$ with surface K-doping level. (a)-(d) Pump-probe signal measured at a delay time of +200 fs on surfaces with K coverage of 0, 0.33, 0.67 and 1 ML, respectively. (e) Curves extracted from the experimental Dirac states for different K dosing time. (f) Evolution of the Dirac point position with K-doping.

Discussion

We shall interpret the above results by recalling a recent experimental and theoretical study [6] where some of us explained the mechanism of formation of the Dirac bands and demonstrated the possibility of tuning the bands by partially substituting Ni for Co in $BaCo_{1-x}Ni_xS_2$. First, by taking into account the non-symmorphic symmetry of the crystal structure, we note that the double degeneracy of the states at M, made of bonding and antibonding combinations of Ni $d-$ and S $p-$ orbitals, is lifted by moving from M to Γ and split by the $p-d$ hybridization. As illustrated in Fig. 4(b), it follows that a Dirac crossing is produced at the Fermi level somewhere along the Γ − M direction between two pairs of states with strong d_{z^2} or $d_{x^2-y^2}$ character, located at M below and above the Fermi level, respectively. Second, by taking into account the x-dependence of the on-site energies and of the charge-transfer gap, Δ_{CT}, i.e. the difference between the average energies of the full d- and p-manifolds, our *ab initio* calculations give an account of the gradual shift of the Dirac nodes towards Γ [6] with decreasing x observed experimentally by ARPES. This is consistent with the general trend that the Δ_{CT} of transition metal compounds increases when moving to elements closer to a half-shell d-manifold, thus leading to a weaker $p-d$ hybridization. [18,19] Indeed, in $BaCo_{1-x}Ni_xS_2$, an increase of Δ_{CT}, i.e. a weaker $p-d$ hybridization, corresponds to a weaker splitting, hence the band crossing moves away from the M point. Finally, we explained the experimental observation of an upward shift in energy of the Dirac cones by noting that the substitution of Ni for Co is equivalent to a bulk hole doping.

The above observations can be applied to the present case of surface doping by electrons, consistent with the experimental observation of a similar k-shift towards Γ and of a downward shift in energy of the Dirac bands. By comparing this result with the previous result on Co-substituted samples, we conclude that electronic doping and momentum shift of the Dirac bands are not directly related. This is understood by considering that the k-shift is governed by Δ_{CT} and that the effect of chemical doping on Δ_{CT} is very different from that of surface doping, as discussed above.

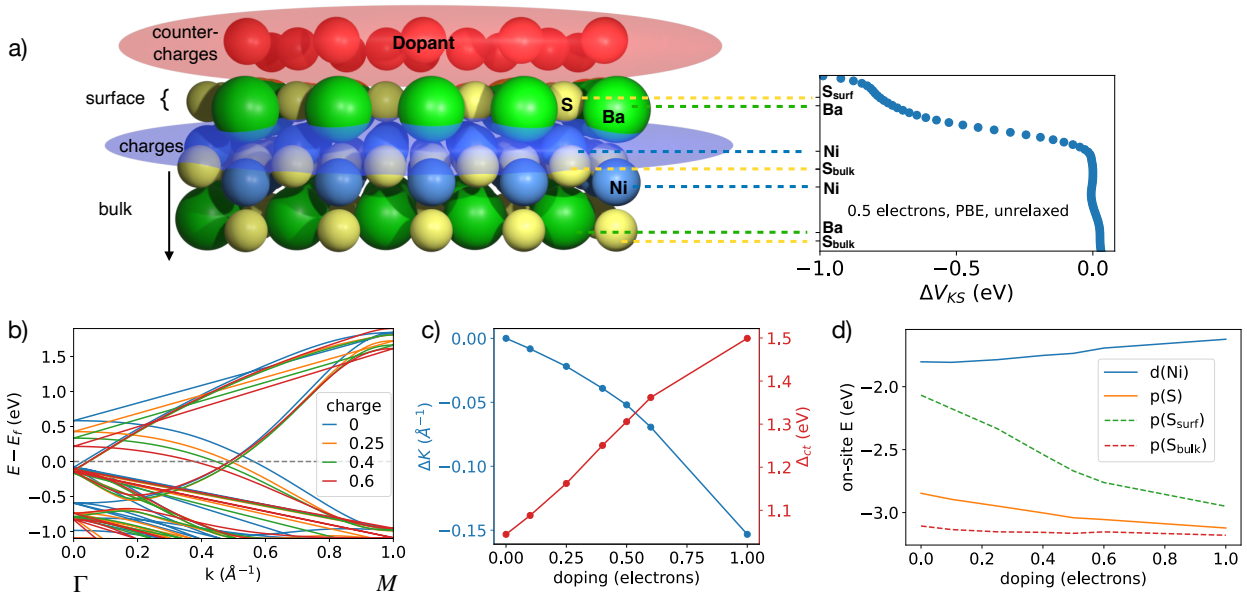

Figure 4: *Ab initio* modeling of the surface doping of $BaNiS_2$. (a) Schematic illustration of the electrostatic effect produced by the K atoms adsorbed on the *ab* surface of $BaNiS_2$. Blue and red regions represent respectively the negatively charged layer of the Ni atoms acceptor of the electrons transferred by the K atoms and the layer of the positively charged K^+ ions at the surface. The top Ba and S layers lie in between these two layers. In the same panel, we also plot the depth profile of the Kohn-Sham potential ΔV_{KS} (i.e. the effective potential probed by the electrons) with respect to the neutral potential for a doping of 0.5 electrons per Ni atom. For technical reasons, this potential was computed using a PBE functional without structural relaxation. (b) Variations of the Wannier band structure as a function of electron doping. (c) Variations in the position of the Dirac cone as well as the charge transfer as a function of doping, as extracted from the Wannier bands. (d) Variations in the on-site energy of Wannier functions associated to Ni and S orbitals, with respect to the Fermi energy. The S *p*-orbitals are decomposed into those of the S atoms at the surface, close to the dopant K atoms, and of the S atoms in the bulk.

In order to account for the above experimental results, we model the doped surface layer as a parallel plate capacitor (see Figure 4(a)), where the top and bottom plates are respectively the layer of the positively charged K^+ ions on the surface and the negatively charged layer of Ni atoms near the surface, acceptor of the electrons donated by the K atoms. The top Ba and S layers of the $BaNiS_2$ unit cell lie in between these two charged layers, while the bottom Ba and S layers of the unit cell, located below the Ni layer, are unaffected by the transverse electric field created by the charged layers and thus behave as in the bulk of the sample. The above field causes a drop of the effective Kohn-Sham potential probed by

the electrons; the on-site energy of the p-orbitals of the surface S atoms drops accordingly, thus increasing the charge transfer gap and shifting the Dirac point towards Γ.

Our *ab initio* calculations on the above capacitor-like model successfully reproduce the experimental observations and support the above intuitive considerations. This is seen in Figures 4(b) and (c) where we show the evolution of the calculated band structure and the position of the Dirac node as a function of electron doping. In 4(c), we plot the increase of the charge transfer gap with increasing electron content, which explains the shift of the Dirac cone towards Γ. The average of the on-site p- and d- orbital energies are presented in Figure 4(d). S_{surf} indicates the S atoms at the surface, located between the charged planes; S_{bulk} are the S atoms in the bulk region, unaffected by the electrostatic field. The corresponding averages on the orbital energies show that the main contribution to the increase of the charge transfer gap is the decrease of the S_{surf} p-orbital energy. Interestingly, in the simplified setup of Figure 4a where the effective potential can be computed, the downward shift of the on-site energy of the p-orbitals of the S_{surf} atoms is found to be 0.86 eV, which matches the potential drop. In conclusion, the *ab initio* results give a full account of the experimental observations and provide a useful estimate of the effective charge transfer from the donor atoms to the substrate (less that one electron per atom).

Conclusion

The present ARPES study supported by first-principles calculations demonstrates the possibility of manipulating the position in reciprocal space of the Dirac states of the layered $BaNiS_2$ semimetal by depositing alkali metals on the sample surface. This simple, clean and controllable method enables to tune directly the physical parameters that control the formation of the Dirac bands in this layered semimetal, namely the $p-d$ hybridization and the charge transfer gap. $BaNiS_2$ appears then to be a promising model system for controlling Dirac electronic states and their functionalization in future electronic devices. More gener-

ally, we envisage that the combination of experimental and theoretical methods employed in the present work is applicable to predict and tune the topological properties of a wide range of materials by injecting appropriate amounts of extra charges in selected atomic layers of nanostructures, surfaces, interfaces and heterostructures.

Methods

Part of the measurements were performed with synchrotron radiation based ARPES: the crystals were freshly cleaved *in situ* within the ab-plane at 100 K in ultra-high vacuum, at a base pressures of 10^{-11} mbar, at the BaDElPh beamline[20] of the Elettra synchrotron in Trieste, Italy, and at the TEMPO beamline of the SOLEIL synchrotron in Saint-Aubin, France. In the former experiment, we used an incident photon energy $h\nu = 26$ eV with a 5 meV photon energy resolution. For the experiments conducted at SOLEIL, the photon energy was 70 eV and the photon energy resolution was better than 10 meV.

For the TR-ARPES experiments, the same high quality single crystals of $BaNiS_2$, grown by a self-flux method were cleaved and kept at a base pressure of about 8×10^{-11} mbar and 130 K during the measurement. The experiments were carried out on the Femto-ARPES setup,[21] using a Ti: Sapphire laser system which delivery 6 μJ pulses with a 250 kHz repetition rate. The laser beam (50 fs pulses, 1.57 eV) were separated into two parts, one used to pump the sample, while the other was employed to generate 6.3 eV photons as a probe pulse.[22] The overall energy resolution of the measurement was about 30 meV, and the cross correlation between pump and probe pulses has a full width at half maximum (FWHM) of 150 fs.

Surface electron doping was realized by deposition of potassium (K) atoms. The evaporations were performed by resistive heating of the getter cartridge (SAES Getters S.p.A.) with typical current values of 4.8-5.2 A. No sample transfer or manipulation were needed between subsequent deposition steps, which minimized the possibility of temperature fluctuations on the sample.

Ab initio simulations are performed with the Quantum ESPRESSO package.[23,24] Only the topmost layer of $BaNiS_2$ is simulated. We use bi-dimensional boundary conditions and the surface dopant is simulated via a uniformly charged plane above the layer.[25] The structure is relaxed at each doping. Following Ref.,[6] Heyd-Scuseria-Ernzerhof (HSE) functionals[26] are used with 7% of exact exchange, which has proven to be optimal by comparing the $BaNiS_2$ band structure with accurate Shubnikov-de Haas and deHaas-van Alphen measurements.[27] The electronic states are sampled with a 8×8 electron-momentum grid in the plane of the layer. The bands are interpolated via Wannier functions using the WANNIER90 code.[28,29] To compute the effective potential of Figure 4a), we had to forgo the use of HSE functionals (to plot the potential) and avoid relaxation, as the atoms displacement makes the comparison between doped and neutral potentials difficult.

Acknowledgement

M.M., L.P. and E.P. work was supported by "Investissement d'avenir Labex Palm" (Grant No. ANR-10-LABX-0039-PALM) and by the ANR "Iridoti" (Grant ANR-13-IS04-0001). J. Z. thanks the China Scholarship Council (CSC) for the financial support. We acknowledge Elettra Sincrotrone Trieste for providing access to its synchrotron radiation facilities.

First-principles calculations were performed with the support of MESO@LR-Platform at the University of Montpellier.

References

(1) Young, S. M.; Kane, C. L. Dirac Semimetals in Two Dimensions. *Phys. Rev. Lett.* **2015**, *115*, 126803.

(2) Lou, R.; Ma, J.-Z.; Xu, Q.-N.; Fu, B.-B.; Kong, L.-Y.; Shi, Y.-G.; Richard, P.; Weng, H.-M.; Fang, Z.; Sun, S.-S.; Wang, Q.; Lei, H.-C.; Qian, T.; Ding, H.; S.-C., W. Emer-

gence of topological bands on the surface of ZrSnTe crystal. *Phys. Rev. B* **2016**, *93*, 241104(R).

(3) Lu, Q.; Cook, J.; Zhang, X.; Chen, K. Y.; Snyder, M.; Nguyen, D. T.; Reddy, P.; Qin, B.; Zhan, S.; Zhao, L.-D., et al. Realization of Unpinned Two-dimensional Dirac States in Antimony Atomic Layers. *Nat. Commun.* **2022**, *13*, 1–8.

(4) Bahramy, M. et al. Ubiquitous formation of bulk Dirac cones and topological surface states from a single orbital manifold in transition-metal dichalcogenides. *Nat. Mater.* **2018**, *17*, 21.

(5) Schoop, L. M.; Ali, M. N.; Strasser, C.; Topp, A.; Varykhalov, A.; Marchenko, D.; Duppel, V.; Parkin, S. P.; Lotsch, B. V.; Ast, C. R. Dirac cone protected by non-symmorphic symmetry and three-dimensional Dirac line node in ZrSiS. *Nat. Commun.* **2016**, *7*, 11696.

(6) Nilforoushan, N. et al. Moving Dirac Nodes by Chemical Substitution. *Proc. Natl. Acad. Sci. U.S.A.* **2021**, *118*, e2108617118.

(7) Santos-Cottin, D.; Casula, M.; Lantz, G.; Klein, Y.; Petaccia, L.; Le Fevre, P.; Bertran, F.; Papalazarou, E.; Marsi, M.; Gauzzi, A. Rashba coupling amplification by a staggered crystal field . *Nat. Commun.* **2016**, *7*, 11258.

(8) Sato, T. e. a. Evolution of metallic states from the Hubbard band in the two-dimensional Mott system BaCo1-xNixS2. *Phys. Rev. B* **2001**, *64*, 075103.

(9) Martinson, L. S.; Schweitzer, J. W.; Baenziger, N. C. Metal-insulator transitions in BaCo1-xNixS2. *Phys. Rev. Lett.* **1993**, *71*, 125.

(10) Krishnakumar, S.; Saha-Dasgupta, T.; Shanthi, N.; Mahadevan, P.; Sarma, D. D. Electronic structure of and covalency driven metal-insulator transition in BaCo1-xNixS2. *Phys. Rev. B* **2001**, *63*, 045111.

(11) Butler, C. J. e. a. Correlation-driven electronic nematicity in the Dirac semimetal BaNiS2. *arxiv:* **2022**, 2207.11920.

(12) Ohtsubo, Y.; Mauchain, J.; Faure, J.; Papalazarou, E.; Marsi, M.; Le Fevre, P.; Bertran, F.; Taleb-Ibrahimi, A.; Perfetti, L. Giant anisotropy of spin-orbit splitting at the bismuth surface. *Phys. Rev. Lett.* **2012**, *109*, 226404.

(13) Huš, M.; Hellman, A. Dipole Effect on Ethylene Epoxidation: Influence of Alkali Metals and Chlorine. *J. Catal.* **2018**, *363*, 18–25.

(14) Pinto, H.; Markevich, A. Electronic and Electrochemical Doping of Graphene by Surface Adsorbates. *Beilstein J. Nanotechnol.* **2014**, *5*, 1842–1848.

(15) Yeh, J. *Atomic Calculation of Photoionization Cross-Section and Asymmetry Parameters*; Gordon & Breach Science: Langhorne, PE (USA), 1993.

(16) Yeh, J.; Lindau, I. Atomic Subshell Photoionization Cross Sections and Asymmetry Parameters: $1 \leq Z \leq 103$. *At. Data Nucl. Data Tables* **1985**, *32*, 1–155.

(17) Nilforoushan, N.; Casula, M.; Caputo, M.; Papalazarou, E.; Caillaux, J.; Chen, Z.; Perfetti, L.; Amaricci, A.; Santos-Cottin, D.; Klein, Y.; Gauzzi, A.; Marsi, M. Moving Dirac Nodes by Chemical Substitution. *Phys. Rev. Research* **2020**, *2*, 043397.

(18) Zaanen, J.; Sawatzky, G. A.; Allen, J. W. Band gaps and electronic structure of transition-metal compounds. *Phys. Rev. Lett.* **1985**, *55*, 418.

(19) Olalde-Velasco, P.; Jimenez-Mier, J.; Denlinger, J. D.; Hussain, Z.; Yang, W. L. Direct probe of Mott-Hubbard to charge-transfer insulator transition and electronic structure evolution in transition-metal systems. *Phys. Rev. B* **2011**, *83*, 241102(R).

(20) Petaccia, L.; Vilmercati, P.; Gorovikov, S.; Barnaba, M.; Bianco, A.; Cocco, D.; Masciovecchio, C.; Goldoni, A. BaD ElPh: A 4 m Normal-Incidence Monochromator Beamline at Elettra. *Nucl. Instrum. Methods Phys. Res. Sect. A* **2009**, *606*, 780.

(21) Faure, J.; Mauchain, J.; Papalazarou, E.; Yan, W.; Pinon, J.; Marsi, M.; Perfetti, L. Full characterization and optimization of a femtosecond ultraviolet laser source for time and angle-resolved photoemission on solid surfaces. *Rev. Sci. Instrum* **2012**, *83*, 043109.

(22) Hajlaoui, M.; Papalazarou, E.; Mauchain, J.; Jiang, Z.; Miotkowski, I.; Chen, Y. P.; Taleb-Ibrahimi, A.; Perfetti, L.; Marsi, M. Time-resolved ultrafast ARPES for the study of topological insulators. *Eur. Phys. J. Special Topics* **2012**, *222*, 1271.

(23) Giannozzi, P. et al. QUANTUM ESPRESSO: A Modular and Open-Source Software Project for Quantum Simulations of Materials. *Journal of Physics: Condensed Matter* **2009**, *21*, 395502.

(24) Giannozzi, P. et al. Advanced Capabilities for Materials Modelling with Quantum ESPRESSO. *Journal of Physics Condensed Matter* **2017**, *29*, 465901.

(25) Sohier, T.; Calandra, M.; Mauri, F. Density Functional Perturbation Theory for Gated Two-Dimensional Heterostructures: Theoretical Developments and Application to Flexural Phonons in Graphene. *Physical Review B* **2017**, *96*, 075448.

(26) Heyd, J.; Scuseria, G. E.; Ernzerhof, M. Hybrid Functionals Based on a Screened Coulomb Potential. *The Journal of Chemical Physics* **2003**, *118*, 8207–8215.

(27) Klein, Y.; Casula, M.; Santos-Cottin, D.; Audouard, A.; Vignolles, D.; Fève, G.; Freulon, V.; Plaçais, B.; Verseils, M.; Yang, H.; Paulatto, L.; Gauzzi, A. Importance of nonlocal electron correlation in the $BaNiS_2$ semimetal from quantum oscillations studies. *Phys. Rev. B* **2018**, *97*, 075140.

(28) Mostofi, A. A.; Yates, J. R.; Pizzi, G.; Lee, Y.-S.; Souza, I.; Vanderbilt, D.; Marzari, N. An Updated Version of Wannier90: A Tool for Obtaining Maximally-Localised Wannier Functions. *Computer Physics Communications* **2014**, *185*, 2309–2310.

(29) Pizzi, G. et al. Wannier90 as a Community Code: New Features and Applications. *Journal of Physics: Condensed Matter* **2020**, *32*, 165902.